Disease Models & Mechanisms 5, 930-939 (2012) doi:10.1242/dmm.008987

The cystic-fibrosis-associated ΔF508 mutation confers post-transcriptional destabilization on the *C. elegans* ABC transporter PGP-3

Liping He[1], Jennifer Skirkanich[1], Lorenza Moronetti[1], Rosemary Lewis[1,2] and Todd Lamitina[1,2,*]

SUMMARY

Membrane proteins make up ~30% of the proteome. During the early stages of maturation, this class of proteins can experience localized misfolding in distinct cellular compartments, such as the cytoplasm, endoplasmic reticulum (ER) lumen and ER membrane. ER quality control (ERQC) mechanisms monitor folding and determine whether a membrane protein is appropriately folded or is misfolded and warrants degradation. ERQC plays crucial roles in human diseases, such as cystic fibrosis, in which deletion of a single amino acid (F508) results in the misfolding and degradation of the cystic fibrosis transmembrane conductance regulator (CFTR) Cl^- channel. We introduced the ΔF508 mutation into *Caenorhabditis elegans* PGP-3, a 12-transmembrane ABC transporter with 15% identity to CFTR. When expressed in intestinal epithelial cells, PGP-3^{wt} was stable and efficiently trafficked to the apical plasma membrane through a COPII-dependent mechanism. However, PGP-$3^{\Delta F508}$ was post-transcriptionally destabilized, resulting in reduced total and apical membrane protein levels. Genetic or physiological activation of the osmotic stress response pathway, which causes accumulation of the chemical chaperone glycerol, stabilized PGP-$3^{\Delta F508}$. Efficient degradation of PGP-$3^{\Delta F508}$ required the function of several *C. elegans* ER-associated degradation (ERAD) homologs, suggesting that destabilization occurs through an ERAD-type mechanism. Our studies show that the ΔF508 mutation causes post-transcriptional destabilization and degradation of PGP-3 in *C. elegans* epithelial cells. This model, combined with the power of *C. elegans* genetics, provides a new opportunity to genetically dissect metazoan ERQC.

INTRODUCTION

Over 30% of all cellular proteins are either secreted or integral membrane proteins. Maturation and folding of this class of proteins is essential for cellular function and this process begins in the endoplasmic reticulum (ER). If proteins fold properly within the ER, they exit this compartment to undergo further post-translational modifications and sorting to their final cellular destination. Proteins that become misfolded in the ER are recognized by ER quality control (ERQC), a system that monitors and manages ER protein biosynthesis (Vembar and Brodsky, 2008). Proteins that are targeted by ERQC can be dealt with through two physiologically distinct pathways. First, they can be refolded through the unfolded protein response (UPR), a multi-faceted stress response that upregulates ER chaperones, increases ER volume and adjusts ER translation to match folding demands (Marciniak and Ron, 2006). Second, they can be degraded through a process called ER-associated degradation (ERAD) (Vembar and Brodsky, 2008). At a molecular level, ERAD is a complex process, requiring chaperones, protein dislocation channel(s), ATPases, ubiquitin conjugating enzymes and proteasome subunits to appropriately recognize, remove and degrade misfolded substrates from the ER membrane and/or lumen (Brodsky and Wojcikiewicz, 2009; Hegde and Ploegh, 2010). Numerous types of misfolding events can activate ERAD, including environmental stressors or genetically encoded mutations in ERQC client proteins (Ward et al., 1995; Kelly et al., 2007). However, even in the absence of environmental or genetic perturbations to protein folding, ERAD is an active process. In some cases, as much as ~75% of newly synthesized proteins are selected for degradation by ERAD owing to errors in protein translation or inappropriate folding trajectories (Varga et al., 2004).

A well-known ERAD substrate is the cystic fibrosis transmembrane conductance regulator (CFTR) (Jensen et al., 1995). CFTR is a 12-transmembrane integral membrane protein of the ABC transporter superfamily. CFTR is only expressed in vertebrates, in which it functions as a cAMP-regulated Cl^- channel in the apical membrane of epithelial cells. Like all ABC transporters, CFTR consists of two transmembrane domains – each with six transmembrane segments – as well as two nucleotide-binding domains (NBD1 and NBD2). In humans, mutations in CFTR cause cystic fibrosis (CF). Although hundreds of disease-causing mutations in CFTR have been documented, the most common is ΔF508, which occurs in NBD1 and is found in ~90% of CFTR mutant alleles (Tsui, 1992). The ΔF508 mutation causes misfolding of CFTR within the ER and subsequent post-transcriptional degradation of most mutant protein by ERAD (Cheng et al., 1990). CFTR$^{\Delta F508}$ degradation by ERAD requires a complex network of interactions between cytosolic and ER lumen chaperones, membrane-localized ubiquitin enzymes, and cytosolic ubiquitin degradation systems (Wang et al., 2006; Younger et al., 2006). ERAD mechanisms have been studied extensively at the cellular and

[1]Department of Physiology, Perelman School of Medicine, and [2]Cell and Molecular Biology Graduate Group, Cell Biology and Physiology Program, University of Pennsylvania, Philadelphia, PA 19104, USA
*Author for correspondence (lamitina@mail.med.upenn.edu)

Received 28 October 2011; Accepted 23 April 2012

biochemical levels, but how these mechanisms operate in an organismal setting is poorly understood.

Although the ΔF508 mutation has a significant effect on CFTR folding, it is also a determinant of protein folding in other ABC transporters. For example, introduction of the ΔF508 mutation into P-glycoprotein (PGP), an ABC transporter closely related to CFTR, disrupts PGP transmembrane packing and maturation within the ER and causes a loss of PGP activity (Loo et al., 2002; Chen et al., 2004). In yeast, ΔF508 inhibits the function of STE6, an ABC transporter required for yeast mating (Teem et al., 1993; Teem et al., 1996) and YOR1, a broad spectrum ABC transporter that mediates drug efflux (Louie et al., 2010; Pagant et al., 2010). Similar to mutant CFTR, efficient degradation of these ABC transporters also requires the function of chaperones, ubiquitin enzymes and other ERAD-associated molecules, suggesting that similar mechanisms govern ERAD-dependent degradation of mutant CFTR and other ABC transporters (Nakatsukasa et al., 2008). Although PGP, YOR1 and STE6 are distinct from CFTR in that they act as transporters and not ion channels, these studies suggest that the ΔF508 mutation within the context of NBD1 is a broad, evolutionarily conserved determinant of ABC transporter protein stability from yeast to humans.

The nematode *Caenorhabditis elegans* is a powerful genetic model system that is used to investigate general mechanisms of protein misfolding and aggregation (Link et al., 2003; Brignull et al., 2006; Cohen et al., 2006; Gidalevitz et al., 2009; Wang et al., 2009). The availability of numerous mutant strains has led to the identification of many unexpected genetic pathways that can influence the folding and toxicity of misfolded substrates (Hsu et al., 2003; Morley and Morimoto, 2004; Garcia et al., 2007). Mechanistic insight into the roles of these pathways is facilitated by the optical transparency of *C. elegans*, which allows the steady-state levels of fluorescently tagged proteins to be visualized with subcellular resolution in live animals from birth until death. In addition to the expected roles for protein chaperones and other cell-autonomous mechanisms that have been previously identified through cell- or biochemistry-based studies, work in *C. elegans* has also identified surprising cell-non-autonomous mechanisms that contribute to cellular protein folding in an organismal context (Garcia et al., 2007; Prahlad et al., 2008; Prahlad and Morimoto, 2011). Although these experimental tools have been applied to models of soluble misfolded proteins (Nollen et al., 2004; Gidalevitz et al., 2009), a *C. elegans* model for membrane protein misfolding in general and/or ΔF508-dependent folding mechanisms has not been developed.

In this study, we developed a misfolded, multipass transmembrane protein in *C. elegans* intestinal epithelial cells by introducing the ΔF508 mutation into the ABC transporter *pgp-3*. Whereas wild-type PGP-3 was stable and trafficked to the apical plasma membrane, PGP-$3^{\Delta F508}$ was unstable and most protein did not reach the plasma membrane. Using PGP-$3^{\Delta F508}$ as an in vivo sensor for membrane protein folding, we found that environmental conditions and genetic pathways that regulate $CFTR^{\Delta F508}$ instability in mammals also regulate PGP-$3^{\Delta F508}$ instability in *C. elegans*. Our studies establish *C. elegans* as a new model system for the study of membrane protein quality control and provide novel opportunities for in vivo genetic, genomic and pharmacological analysis of this complex process in animals.

RESULTS

The ΔF508 mutation post-transcriptionally destabilizes PGP-3 in *C. elegans*

In mammals, the CFTR protein is an important representative model for the study of membrane protein folding and quality control systems (Peters et al., 2011). Although CFTR homologs are present throughout vertebrate genomes, they are absent from the genomes of invertebrates, such as *C. elegans*. However, CFTR is a member of the ABC transporter gene family, of which there are at least 60 *C. elegans* homologs (Sheps et al., 2004; Zhao et al., 2004; Zhao et al., 2007). In total, 14 of these ABC transporters encode PGPs, proteins that have been used previously to model ΔF508 folding defects in mammalian cells (Loo et al., 2002; Chen et al., 2004). *C. elegans* PGP proteins exhibit 13-16% identity with human CFTR (supplementary material Table S1). Most of this homology is found within the highly conserved NBD1 and NBD2 domains (supplementary material Fig. S1). In human CFTR, the F508 mutation lies within the NBD1 domain (~amino acids 433-586 of human CFTR). To model ΔF508 folding defects in worms, we searched for a *C. elegans* PGP with qualities similar to those of mammalian CFTR, namely one that is expressed in epithelial cells and that is trafficked to the apical plasma membrane. Previous studies have shown that PGP-3 exhibits these properties (Lincke et al., 1993; Broeks et al., 1995). However, PGP-3 is functionally distinct from CFTR in that it functions as an ATP-dependent drug transporter and not as a cAMP-activated Cl^- channel (Lincke et al., 1993; Broeks et al., 1995). We cloned *pgp-3* and replaced a nine-amino-acid-encoding region (amino acids 476-484) within NBD1 with a homologous human CFTR sequence surrounding F508 (amino acids 501-509), as had been previously done with human PGP (*pgp-*3^{wt}) (Loo et al., 2002) (Fig. 1A). We also created a variant that lacked the F508 residue (*pgp-*$3^{\Delta F508}$). The expression of both constructs was driven by the *vha-6* promoter, which is active only in polarized intestinal epithelial cells (Oka et al., 2001; Allman et al., 2009). The proteins were tagged at the N-terminus with a 3×FLAG epitope and at the C-terminus with mCherry. In the intestine, the tagged proteins were functional, as measured by the ability to rescue the slow growth phenotype of *pgp-1(pk17); pgp-3(pk18)* double-mutant animals (supplementary material Fig. S2). The transgenes were integrated into the same genomic location at single-copy level using the Mos-mediated transgene insertion method (Frokjaer-Jensen et al., 2008). As expected for single-copy insertions, quantitative PCR showed that the mRNA for both *pgp-*3^{wt} and *pgp-*$3^{\Delta F508}$ was expressed at identical levels (Fig. 1B). Similar results were obtained with extrachromosomal array and integrated overexpression lines (supplementary material Fig. S3).

In the intestine, PGP-3^{wt} was trafficked to the apical plasma membrane (Fig. 1C). Trafficking of PGP-3^{wt} occurred through a COPII-dependent pathway, because RNA interference (RNAi) of *C. elegans sec-24.1*, a homolog of yeast *sec24*, which is required for the trafficking of proteins from the ER to the Golgi (Barlowe et al., 1994), strongly attenuated overall abundance and apical membrane localization of PGP-3^{wt} (supplementary material Fig. S4). Compared with PGP-3^{wt}, the steady-state fluorescence of the PGP-$3^{\Delta F508}$ protein was significantly reduced (Fig. 1C). Quantitative analysis of mCherry fluorescence showed that there was significantly reduced total fluorescence and reduced apical membrane fluorescence for PGP-$3^{\Delta F508}$ compared with PGP-3^{wt} (Fig. 1D), although image

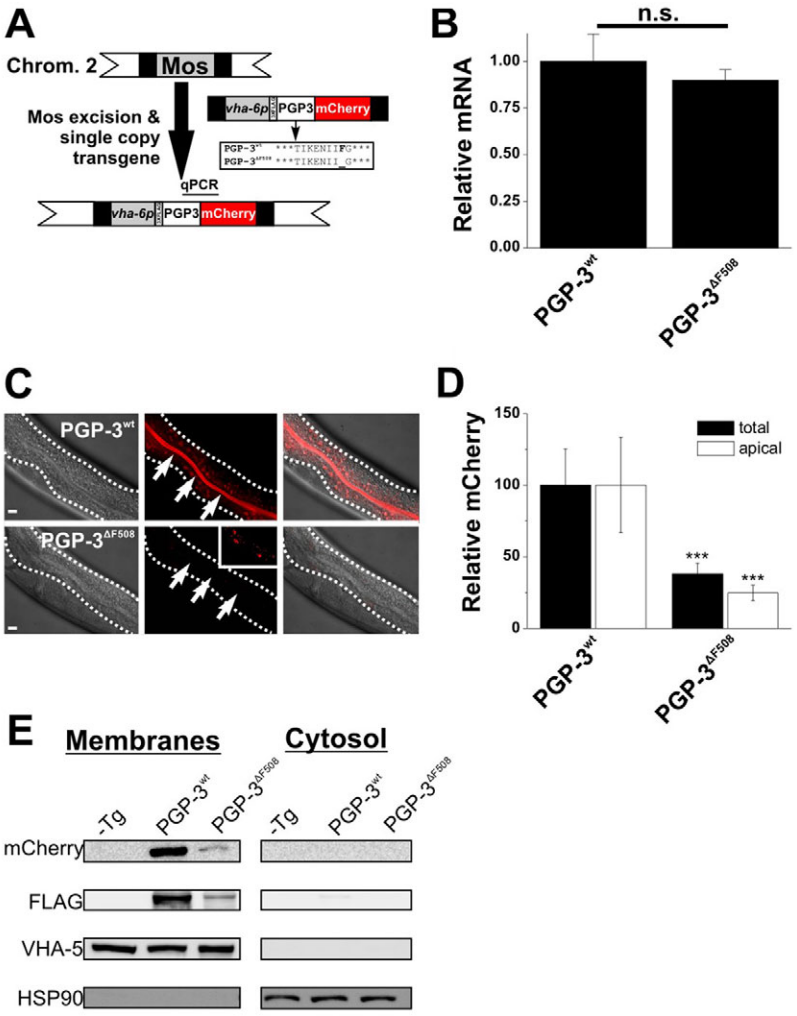

Fig. 1. The ΔF508 mutation post-transcriptionally destabilizes the abundance and apical membrane localization of *C. elegans* PGP-3. (A) Schematic of the Mos excision strategy used to create the single-copy PGP-3^{wt} and PGP-3$^{\Delta F508}$ transgenes. (B) Quantitative PCR of the *pgp-3*–mCherry transgenic mRNA. As shown in A, the primers only amplify the transgenic *pgp-3* and not the native *pgp-3*. n=4 samples, P>0.05. (C) In vivo localization of the PGP-3^{wt}::mCherry and PGP-3$^{\Delta F508}$::mCherry protein in intestinal epithelial cells. Arrows indicate the apical membrane of the intestine. Dotted lines denote the basolateral membranes of the intestine. Imaging settings for both lines are identical. Inset image has been adjusted for intensity and contrast to show the presence of a weak signal in the PGP-3$^{\Delta F508}$ animals. Scale bars: 10 μm. (D) Quantification of total and apical intestinal mCherry fluorescence from PGP-3^{wt}::mCherry or PGP-3$^{\Delta F508}$::mCherry single-copy transgenes. ***P<0.001. n=12 (PGP-3^{wt}) or 13 (PGP-3$^{\Delta F508}$). (E) Western blot against transgenic PGP-3 (mCherry and FLAG antibodies), a positive control membrane protein (VHA-5) and a positive control cytosolic protein (HSP-90). Membrane and cytosolic fractions were prepared from single-copy transgenic animals as described in the Methods. '-Tg' indicates animals that lack the single copy transgene.

enhancement showed that some PGP-3$^{\Delta F508}$::mCherry protein could be detected at or near the apical membrane (supplementary material Fig. S5). Given that ΔF508 is known to cause protein misfolding, we considered the possibility that the apparent reduction in fluorescence was due to global misfolding of the PGP-3$^{\Delta F508}$ protein and the linked mCherry reporter. However, this was not the case: western blot analysis confirmed a reduction in PGP-3$^{\Delta F508}$ protein levels compared with PGP-3^{wt} (Fig. 1E). Furthermore, in extrachromosomal array lines, which exhibit highly variable expression levels, the slope of the mRNA:fluorescence relationship was substantially reduced in PGP-3$^{\Delta F508}$ animals as compared with PGP-3^{wt} animals (supplementary material Fig. S3). Together, these data show that *C. elegans* PGP-3 is a COPII-trafficked membrane protein and that introduction of the ΔF508 mutation into NBD1 causes a post-transcriptional reduction in both the overall steady-state levels and apical membrane abundance of PGP-3.

Genetic or physiological activation of the osmotic stress response stabilizes PGP-3$^{\Delta F508}$

In mammalian cells, CFTR$^{\Delta F508}$ can be stabilized following exposure of cells to either low temperature or high levels of glycerol or other organic osmolytes (Sato et al., 1996; Howard et al., 2003). We investigated whether exposure of worms to these conditions might similarly stabilize PGP-3$^{\Delta F508}$. Worms exposed to either low temperature (growth at 15°C or 24-hour exposure to 4°C; data not shown) or high temperature (1-hour exposure to 35°C heat shock; supplementary material Fig. S6) did not exhibit significantly altered expression levels of PGP-3$^{\Delta F508}$. However, exposure of worms to hyperosmotic environments, which stimulates the synthesis and accumulation of the osmolyte glycerol in the intestine (Lamitina et al., 2004; Lamitina et al., 2006; Rohlfing et al., 2010; Rohlfing et al., 2011), significantly stabilized PGP-3$^{\Delta F508}$ total and apical membrane fluorescence (Fig. 2). Hyperosmotic stress also increased the abundance and apical membrane localization of PGP-3^{wt}, although, unlike PGP-3$^{\Delta F508}$, PGP-3^{wt} stabilization was not strong enough to be detected by western blot analysis (Fig. 2). mRNA levels for PGP-3, as measured by qPCR, were not affected by hyperosmotic stress (supplementary material Fig. S7). These data show that physiological activation of the osmotic stress response (Osr) pathway, but not other stress response pathways, post-transcriptionally stabilizes PGP-3$^{\Delta F508}$ in *C. elegans*.

We also examined whether genetic activation of known protein folding pathways improved PGP-3$^{\Delta F508}$ stability. Mutations in both the *daf-2*–IGF (insulin-like growth factor) signaling pathway and the Osr pathway protect against related but distinct types of protein misfolding and aggregation in *C. elegans* (Hsu et al., 2003;

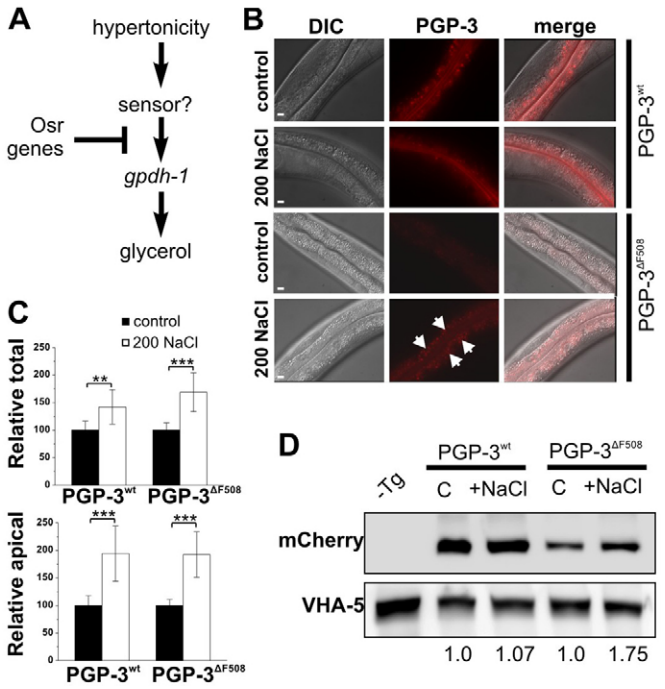

Fig. 2. Physiological activation of the osmotic stress response post-transcriptionally stabilizes PGP-3$^{\Delta F508}$ and PGP-3^{wt}. (A) Genetics of the Osr pathway. Arrows indicate positive regulation and blocked lines indicate negative regulation, based on previous research (Solomon et al., 2004; Lamitina et al., 2006; Wheeler and Thomas, 2006; Rohlfing et al., 2010; Rohlfing et al., 2011); loss-of-function mutations in the Osr genes result in constitutive activation of the pathway even under isotonic conditions. (B) Wide-field fluorescence images of PGP-3-mCherry grown on standard NGM plates (control) or high salt plates (200 mM NaCl, 24-hour exposure). Exposure and imaging settings were identical across all conditions. Arrows indicate sites of increased intestine expression in high-salt-treated PGP-3$^{\Delta F508}$ animals. Scale bars: 10 μm. (C) Quantification of total and apical membrane fluorescence from animals grown on 50 mM NaCl or 200 mM NaCl growth plates. Data for both PGP-3^{wt} and PGP-3$^{\Delta F508}$ are normalized relative to the isotonic (50 mM NaCl) control. $^{**}P<0.01$, $^{***}P<0.001$, one-way ANOVA. (D) Representative western blot of synchronized young adult PGP-3^{wt} or PGP-3$^{\Delta F508}$ grown on either control (50 mM NaCl) or +NaCl (200 mM NaCl) NGM media. PGP-3 was detected with an anti-mCherry antibody. The numbers beneath each lane represent the normalized PGP-3:actin ratio for the experiment shown. One of four representative experiments is shown.

Moronetti Mazzeo et al., 2012). Therefore, we tested whether activation of these pathways might stabilize PGP-3$^{\Delta F508}$. We found that *daf-2(e1370)* mutants had no effect on the stability or trafficking of PGP-3$^{\Delta F508}$ (supplementary material Fig. S8). However, Osr mutants, such as *osm-7* or *osm-11*, significantly improved the stability of PGP-3$^{\Delta F508}$ (Fig. 3). Osr mutants increased both the total amount of PGP-3$^{\Delta F508}$ protein as well as the amount of protein that was trafficked to the apical plasma membrane (Fig. 3). As was the case during hyperosmotic adaptation, Osr mutants also stabilized PGP-3^{wt}. Together, these data show that PGP-3$^{\Delta F508}$ stability can be regulated by genetic and physiological activation of the Osr pathway but not by other pathways known to regulate protein folding, such as the insulin/IGF pathway. Because IGF signaling is known to suppress the folding defects associated with other non-membrane-localized substrates (Hsu et al., 2003; Morley and Morimoto, 2004), these data suggest that the genetic mechanisms regulating the folding and stability of the PGP-3$^{\Delta F508}$ membrane protein are distinct from those regulating the folding of previously described cytosolic substrates in *C. elegans*.

Destabilization of PGP-3$^{\Delta F508}$ is dependent on *C. elegans* ERAD homologs

Misfolded membrane proteins within the ER trigger ERAD, an evolutionarily conserved degradation pathway. Genetic studies in yeast and biochemical studies in mammalian cells have identified several evolutionarily conserved proteins that play key roles in ERAD (Vembar and Brodsky, 2008). We identified *C. elegans* homologs for many ERAD genes based on sequence homology (Table 1) and examined their roles in the regulation of PGP-3$^{\Delta F508}$ and PGP-3^{wt} stability in vivo using RNAi (for genes whose mutant phenotype is lethal or for genes without an available mutation) or available loss-of-function mutants to knock down gene expression. Previous studies have suggested that the Derlin proteins play important roles in ERAD (Ye et al., 2004; Younger et al., 2006; Schaheen et al., 2009), as well as in the trafficking and degradation of misfolded plasma membrane proteins (Dang et al., 2011). *C. elegans* contains two Derlin homologs, *cup-2* and *R151.6* (*der-2*), homologous to Derlin-1 and Derlin-2, respectively. *cup-2* mutants were previously shown to increase the abundance of some membrane proteins, as well as to cause the activation of the UPR (Ye et al., 2004; Schaheen et al., 2009). The function of R151.6 is unknown. We found that both *R151.6(RNAi)* and *cup-2(ar506)* loss-of-function mutants increased total and apical membrane protein levels of PGP-3$^{\Delta F508}$. However, these RNAi knockdowns had no effect on the steady-state levels of PGP-3^{wt} (Fig. 4, Table 1; supplementary material Table S2). In addition to the Derlin proteins, we also discovered a role for Cdc48 (p97) homologs in the degradation of PGP-3$^{\Delta F508}$. The Cdc48 genes encode AAA ATPases that are required for ERAD in both yeast and mammalian cells (Huyer et al., 2004; Goder et al., 2008; Nakatsukasa et al., 2008). *C. elegans* expresses three Cdc48 homologs, *cdc-48.1*, *cdc-48.2* and *cdc-48.3*. We found that post-embryonic RNAi inhibition of *cdc-48.1* and *cdc-48.2*, but not *cdc-48.3*, increased total and apical levels of PGP-3$^{\Delta F508}$ but had little effect on PGP-3^{wt} (Fig. 4, Table 1; supplementary material Table S2). Functional inhibition of other ERAD regulators, including the ER chaperone calreticulin, and the RING finger E3 ubiquitin ligase *rnf-5*, also weakly stabilized PGP-3$^{\Delta F508}$ (Table 1; supplementary material Table S2). Together, these data show that the reduction in PGP-3$^{\Delta F508}$ protein requires the activity of *C. elegans* ERAD homologs and suggest that PGP-3$^{\Delta F508}$ is degraded through an ERAD-type mechanism.

DISCUSSION

The ΔF508 mutation is a critical regulator of protein stability in CFTR and other ABC transporters across a wide range of species. Analyses of the pathways that participate in ΔF508 substrate recognition and degradation have mostly been limited to biochemical approaches in single cells. Here, we introduce a *C. elegans* model that allows investigation of ΔF508-dependent recognition and degradation mechanisms in a multicellular, live-animal, epithelial tissue setting. Using genetic approaches, we show that proteins with well-established roles in ERAD-type degradation contribute to the degradation of PGP-3$^{\Delta F508}$ in *C. elegans*. Furthermore, we show that

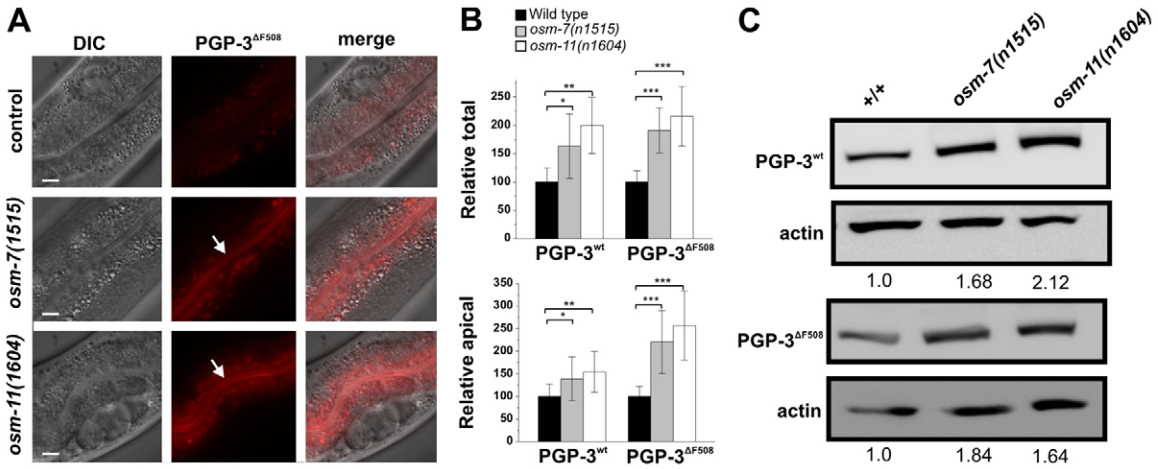

Fig. 3. Genetic activation of the Osr pathway stabilizes PGP-3$^{\Delta F508}$ and PGP-3^{wt}. (A) DIC and wide-field fluorescence images of PGP-3$^{\Delta F508}$ in the indicated Osr mutant backgrounds grown on standard (50 mM NaCl) NGM plates. Arrows point to sites of PGP-3$^{\Delta F508}$ apical membrane localization. Scale bars: 10 µm. (B) Quantification of total and apical membrane fluorescence from animals expressing PGP-3$^{\Delta F508}$ or PGP-3^{wt} in the indicated genetic background. Data are normalized relative to the wild-type control. *P<0.05, **P<0.01, ***P<0.001, one-way ANOVA. (C) Representative western blot of PGP-3$^{\Delta F508}$ and PGP-3^{wt} in the indicated genetic background. The numbers beneath each set of images represent the normalized PGP-3:actin ratio for the experiment shown. One of two representative experiments is shown.

a physiologically significant stress response pathway can be leveraged to ameliorate the folding defects caused by ΔF508 in vivo. Other in vivo transgenic models of ΔF508-mediated misfolding have been developed in animal model systems, including pigs, ferrets and mice (Stoltz et al., 2010; Sun et al., 2010; Ostedgaard et al., 2011; Wilke et al., 2011), and these systems permit detailed analysis of ΔF508-associated pathophysiology. However, none of the models permit the application of high-throughput genetic screening approaches, which is the major strength of the *C. elegans* system. It is important to note that *C. elegans* PGP-3 probably exhibits different functional characteristics from human CFTR, because PGP-3 is a transporter whereas CFTR is an ion channel. Moreover, our *C. elegans* ΔF508 model does not recapitulate certain clinically important aspects of ΔF508-associated tissue pathophysiology, such as progressive and chronic lung infection, because worms do not have airway epithelia. However, our studies show that the ΔF508 mutation does reproduce the general molecular pathophysiology of CF. Given the power of *C. elegans* genetics, this model offers an opportunity to dissect the underlying genetic mechanisms that contribute to ΔF508 instability using unbiased forward and reverse genetic screens and PGP-3$^{\Delta F508}$::mCherry fluorescent stability as a phenotype. In support of the feasibility of this approach, we have recently carried out forward genetic screens and identified several mutants with enhanced PGP-3$^{\Delta F508}$ protein levels that do not significantly alter mRNA levels (data not shown). The stabilization observed in these mutants is substantially higher than that seen following inhibition of ERAD genes or activation of the Osr pathway, suggesting that they affect a distinct pathway. Such in vivo genetic screening approaches for regulators of ΔF508 protein stability are not yet technically or financially practical using other in vivo model systems. The evolutionary position of *C. elegans* in relation to yeast and mammals could provide new insights into membrane protein quality control that cannot be revealed through either yeast or mammalian studies on their own.

In humans, the ΔF508 mutation reduces the abundance of the CFTR protein to levels that are insufficient to support its function. Likewise, introduction of ΔF508 into the yeast ABC transporters Ste6p and Yor1p also inhibits the function of these ABC transporters (Teem et al., 1993; Pagant et al., 2007). Surprisingly, we found that, although introduction of ΔF508 into *C. elegans* PGP-3 leads to post-transcriptional protein destabilization, PGP-3$^{\Delta F508}$ is still functional, as measured by its ability to rescue *pgp-1; pgp-3* double mutants (supplementary material Fig. S2). PGP-3$^{\Delta F508}$ also rescued *pgp-1; pgp-3* mutants when expressed under the less active *pgp-3* promoter at single-copy level, even though this promoter reduced total and apical expression by ~80% and preserved the post-transcriptional reductions in PGP-3$^{\Delta F508}$ protein levels observed with the *vha-6* promoter (data not shown). Why might this PGP-3$^{\Delta F508}$ protein be functional in *C. elegans*? One possible explanation is that, although PGP-3$^{\Delta F508}$ protein levels are reduced, they are still at or above the levels needed to provide function. Although the ΔF508 mutation virtually eliminates all functional CFTR protein from human airway epithelial cells, it has a substantially weaker effect on CFTR in other tissues and organisms (Ostedgaard et al., 2007; Luo et al., 2009; van Barneveld et al., 2010). Moreover, data from human airway epithelia suggest that only 25% of normal CFTR function is needed to rescue epithelial defects (Zhang et al., 2009). In *C. elegans*, PGP-3$^{\Delta F508}$ levels are ~20% that of PGP-3^{wt} (Fig. 1). By these criteria, there might still be a sufficient level of protein to rescue *pgp-3* mutant phenotypes in our *C. elegans* model. Although these findings currently preclude us from determining whether treatments that stabilize PGP-3$^{\Delta F508}$ also improve function, these data do show that the PGP-3$^{\Delta F508}$ protein in *C. elegans*, like CFTR$^{\Delta F508}$ in humans, is active. The development of PGP-3 transgenes under the control of weaker promoters, as well as the development of new ERQC substrates, should eventually provide assays that allow us to examine both substrate function and stability.

Table 1. *C. elegans* ERAD homologs and effect of their gene knockdown on PGP-3$^{\Delta F508}$ expression

Yeast	Mammals	*C. elegans*[a]	Affects PGP3$^{\Delta F508}$ total expression[b]	Affects PGP3$^{\Delta F508}$ apical expression[b]	Affects PGP3^{WT} total expression[b]	Affects PGP3^{WT} apical expression[b]
Recognition						
Bip/Kar2	*GRP78/Bip*	*hsp-3*/C15H9.6[c,d]	–	–	N.D.	N.D.
		hsp-4/F43E2.8	N.D.	N.D.	N.D.	N.D.
Cne1	Calnexin	*cnx-1*/ZK632.6[c]	–	–	N.D.	N.D.
–	Calreticulin	*crt-1*/Y38A10A.5[d]	++	+	–	–
Aha1	*Aha1*	C01G10.8	N.D.	N.D.	N.D.	N.D.
Retrotranslocation						
Sec61	*Sec-61*	Y57G11C.15	N.D.	N.D.	N.D.	N.D.
Der1	Derlin-1, -2, -3	*cup-2*/F25D7.1[c,d]	+	+	N.D.	N.D.
		R151.6[d]	++	++	–	–
Cdc48	*p97*	*cdc-48.1*/C06A1.1[d]	+++	+++	N.D.	N.D.
		cdc-48.2/C41C4.8[d]	+++	+++	–	–
		cdc-48.3/K04G2.3[d]	–	–	–	–
Ubiquitylation						
Uba1	*UBE1*	*uba-1*/C47E12.5	N.D.	N.D.	N.D.	N.D.
Hrd1/3	*HRD1/SEC1*	*sel-1*/F45D3.5	N.D.	N.D.	N.D.	N.D.
		sel-11/F55A11.3	N.D.	N.D.	N.D.	N.D.
Doa10	*TEB4*	*marc-6*/F55A3.1[d]	–	–	N.D.	N.D.
??	*RMA1/GRP78/RNF5*	*rnf-5*/C16C10.7[c]	+	+	N.D.	N.D.
Rsp5	*Nedd4-2*	*wwp-1*/Y65B4BR.4[d]	–	–	N.D.	N.D.
Degradation						
–	*RPN10/RPN13/RPT5*	*rpt-5*/F56H1.4	N.D.	N.D.	N.D.	N.D.
–	–	*rpt-6*/Y49E10.1[d]	–	–	N.D.	N.D.

Homologs have been grouped into predicted molecular functions, based on previous literature.

[a]Homology to known ERAD genes was determined by sequence analysis and BLAST searches. Gene names/sequence names are as indicated in Wormbase.

[b]N.D., gene not tested; –, no statistically significant effect of ≥25% on PGP-3$^{\Delta F508}$ levels (P>0.05, ANOVA with Dunnett's post-test); +, 25-50% increase in PGP-3$^{\Delta F508}$ levels; ++, 50-100% increase in PGP-3$^{\Delta F508}$ levels; +++, >100% increase in PGP-3$^{\Delta F508}$ levels. +, ++ and +++ were all significant at P<0.05 (ANOVA with Dunnett's post-test). Detailed quantification and statistics for individual experiments can be found in supplementary material Table S1.

[c]Tested by using a loss-of-function mutant.

[d]Tested by using RNAi.

Our findings reveal an important role for the Osr pathway in the regulation of PGP-3$^{\Delta F508}$ stability. We found that activation of this pathway, either through physiological or genetic mechanisms, stabilizes PGP-3$^{\Delta F508}$ in the intestine. Activation of other proteotoxic stress pathways, including the *hsf-1*-dependent heat-shock response and the longevity-promoting IGF signaling pathway, did not alter PGP-3$^{\Delta F508}$ stability, suggesting that the specific physiological targets of osmotic stress stabilize PGP-3$^{\Delta F508}$. A primary physiological role of the osmotic stress pathway is to direct the accumulation of the organic osmolyte glycerol (Lamitina et al., 2004; Rohlfing et al., 2010). Although mammalian cells do not utilize glycerol as an organic osmolyte during osmotic adaptation, exogenous glycerol is a well-known stabilizer of CFTR$^{\Delta F508}$ in mammalian cells (Sato et al., 1996). In the mammalian kidney, osmotic adaptation induces the accumulation of several organic osmolyte species. Interestingly, CFTR$^{\Delta F508}$ exhibits normal stability and trafficking in renal epithelial cells, suggesting that osmolytes might also act as a stabilizer of CFTR$^{\Delta F508}$ misfolding and degradation in this tissue (Howard et al., 2003). Together, these data point to an important and conserved role for osmolytes in the stabilization of misfolded membrane proteins. The activation of such genetically regulated osmolyte biosynthesis pathways could be used therapeutically to improve CFTR folding in vivo. Although there are many physiological arguments against this strategy, the isolation of mutant *C. elegans* with this phenotype and observation that these animals appear relatively normal (Wheeler and Thomas, 2006; Rohlfing et al., 2011) suggest that this strategy may be feasible. In this respect, an important future goal is to test whether similar mechanisms for genetic activation of the Osr pathway exist in mammals and whether activation of these pathways improves CFTR$^{\Delta F508}$ folding in different cellular contexts, including in the lung.

We also found that PGP-3$^{\Delta F508}$ degradation depends on the activity of *C. elegans* ERAD homologs. RNAi knockdown of *C. elegans* homologs of Derlins, *cdc-48*, Calreticulin and *rnf-5* all reproducibly stabilized PGP-3$^{\Delta F508}$ but not PGP-3^{wt}, suggesting that these ERAD homologs exhibit specific interactions with the destabilized substrate. We also tested whether PGP-3$^{\Delta F508}$ stability was dependent on the proteasome, because all ERAD substrates in yeast are degraded to varying extents by the proteasome (Vembar

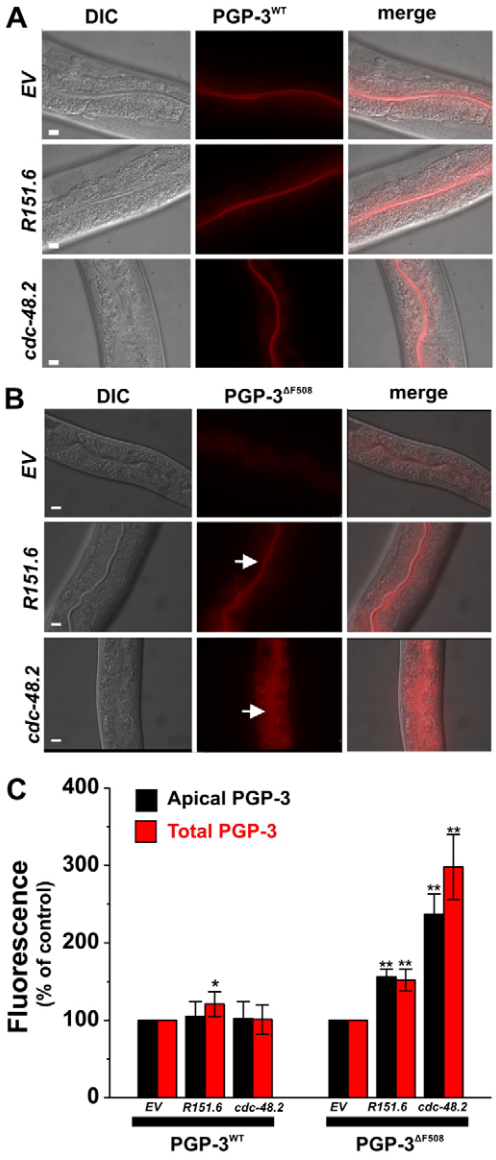

Fig. 4. ERAD homologs are required to efficiently destabilize PGP-3$^{\Delta F508}$ but not PGP-3^{wt}. (A) PGP-3^{wt}::mCherry fluorescence following RNAi inhibition of *R151.6* (Derlin 2) or *cdc-48.2* (p97). EV, empty vector. Scale bars: 10 µm. (B) PGP-3$^{\Delta F508}$::mCherry fluorescence following RNAi inhibition of *R151.6* or *cdc-48.2*. Scale bars: 10 µm. Arrows point to sites of enriched apical mCherry expression. (C) Quantification of apical and total PGP-3^{wt} (young adults) or PGP-3$^{\Delta F508}$ (L4 stage) mCherry fluorescence following the indicated RNAi treatments. Data are normalized to the empty vector control and exposure settings within the PGP^{wt} and PGP-3$^{\Delta F508}$ test groups were identical. Data shown represent the mean ± s.d. of one representative experiment. **P*<0.05, ***P*<0.01, one-way ANOVA. *n*=9-16 animals per condition.

and Brodsky, 2008). However, neither pharmacological (MG-132 inhibition) nor reverse genetic approaches (RNAi against proteasome genes) to inhibit proteasome activity significantly stabilized PGP-3$^{\Delta F508}$ protein levels (data not shown). This could be because PGP-3$^{\Delta F508}$ degradation can occur through proteasome-independent mechanisms (Donoso et al., 2005) or because our manipulations failed to sufficiently inhibit proteasome activity or selected for animals with minimally affected activity. Yet another possibility is that proteasome inhibition does in fact stabilize PGP-3$^{\Delta F508}$, but also simultaneously inhibits PGP-3$^{\Delta F508}$ protein synthesis through activation of the PERK branch of the UPR, resulting in no net increase in steady-state PGP-3$^{\Delta F508}$ protein levels. Notably, the PERK branch of the UPR is not found in yeast, in which, in contrast to animals, protein synthesis continues during ER stress and proteasome inhibition strongly stabilizes ERAD substrates (Mori, 2009). In this respect, *C. elegans*, which contains all major branches of the UPR, could provide an important animal-specific platform to investigate in vivo integration of ER stress responses and ERAD mechanisms with single-cell resolution in a way that is not possible in yeast.

In conclusion, we have developed a *C. elegans* model that recapitulates post-transcriptional ΔF508-dependent membrane protein instability. In addition to the expected roles for ERAD homologs, our system also identified an important and specific function for the Osr pathway in stabilizing PGP-3$^{\Delta F508}$. Given the simple fluorescent phenotype caused by PGP-3$^{\Delta F508}$ and the amenability of *C. elegans* to forward genetic screening, this system offers a new opportunity to dissect the genetics and genomics of ΔF508-dependent membrane protein misfolding in a way that was not previously possible. Such studies could provide unique insight into the mechanistic underpinnings of ΔF508-dependent membrane protein misfolding and instability, as well as suggest novel in vivo approaches for the treatment of protein misfolding diseases.

METHODS

C. elegans strains

The following strains were utilized; EG4322–unc-119(ed3); ttTi5605 (Mos1), GS2555–cup-2(ar506); arIS37; dpy-20(e1282), RB922–rnf-5(ok793), RB1104–hsp-3(ok1083), VC1801–cnx-1(ok2234), CB1370–daf-2(e1370), MT3564–osm-7(n1515), MT3643–osm-11(n1604), drSi2[Cbunc-119+, vha-6p::3×FLAG-pgp-3(CFTR^{wt})-mCherry::unc-54], drSi5 [Cbunc-119+, vha-6p::3×FLAG-pgp-3(CFTR$^{\Delta F508}$)-mCherry::unc-54]. Standard genetic crossing methods (Brenner, 1974) were used to place mutants into the drSi2 or drSi5 backgrounds. Mutant genotypes were confirmed by PCR (for deletion alleles), DNA sequencing or phenotypic analysis.

Molecular biology and transgenics

To generate the *pgp-3* expression clones, we first amplified (Expand High-Fidelity Polymerase, Roche) the *pgp-3* genomic interval (lacking start and stop codons and containing introns) from wild-type genomic DNA with primers containing attB1 and attB2 Gateway recombination sites. The resulting PCR product was recombined with pDONR221 to generate pENTRY-*pgp-3*. pENTRY-*pgp-3*^{wt} and -*pgp-3*$^{\Delta F508}$ were created using a PCR fusion strategy using pENTRY-*pgp-3* as the template. Briefly, a 5′ fragment, in which the 3′ primer (OG496 or OG501) replaced amino acids 476-484 of *pgp-3* with amino acids 501-509 of human CFTR (with or without F508) was amplified from pENTRY-*pgp-3*. A second 3′ overlapping fragment was amplified from pENTRY-*pgp-3*. The 5′ and 3′ PCR fragments were then fused using primers flanking *Age*I and *Kpn*I sites in *pgp-3*. The fusion PCR product was digested with *Age*I and *Kpn*I and used to replace the *Age*I-*Kpn*I fragment in pENTRY-*pgp-3*. The N-terminal 3×FLAG tag was added to pENTRY-*pgp-3*^{wt} and pENTRY-

pgp-3$^{\Delta F508}$ using a PCR fusion approach. A 5′ fragment that flanked the *Apa*I site and that contained the 3×FLAG sequence (DYKDHDGDYKDHDIDYKDDDDK) was fused with a 3′ fragment that flanked an *Asc*I site. The fusion product was digested with *Apa*I and *Asc*I and ligated into either pENTRY-*pgp-3*^{wt} or pENTRY-*pgp-3*$^{\Delta F508}$ to generate pENTRY-3×FLAG-*pgp-3*^{wt} or pENTRY-3×FLAG-*pgp-3*$^{\Delta F508}$, respectively. The mCherry–*unc-54* 3′UTR was amplified from MB14-mCherry with primers containing attB2r and attB3, then recombined with pDONOR P2rP3. MB14-mCherry was created by replacing the GFP region of MB14 (kind gift of Denis Dupuy, Institut Européen de Chemie et Biologie, France) with mCherry cDNA. The 3×FLAG sequence and the human CFTR sequences were codon-optimized for expression in *C. elegans* (Duret and Mouchiroud, 1999). PCR-induced mutations were corrected using site-directed mutagenesis and the sequence of all final entry clones was verified by DNA sequencing.

Expression clones for transgene construction (see below) were generated using Multisite Gateway technology. The promoter clone pENTRY-*vha-6p*, the relevant pENTRY-*pgp-3* clone, and pENTRY-mCherry-*unc-54*-3′UTR were recombined in a Gateway LR reaction with pCFJ150 (Frokjaer-Jensen et al., 2008). The resulting expression clones were validated by restriction digest analysis and DNA sequencing.

Mos-mediated single-copy transgenes were created as previously described, utilizing the ttTi5605 Mos site on chromosome II and the direct-insertion screening method (Frokjaer-Jensen et al., 2008). Approximately 40 P0 young adults from the strain EG4322 *unc-119(ed3); ttTi5605* were injected with each *pgp-3* expression construct and the standard concentrations of co-injection markers (Frokjaer-Jensen et al., 2008). After 12-14 days, animals that exhibited normal motility but lacked the mCherry co-injection markers were isolated as candidate insertion lines. To verify that the insertion was present at single-copy level, candidate insertions were made homozygous for the insertion and long-range PCR (Long-Amp system, New England Biolabs) was performed across the genomic interval using purified genomic DNA and primers outside of the recombination interval. Products of the correct size were further analyzed by restriction digest analysis.

Quantitative PCR

Quantitative PCR was carried out as described previously (Rohlfing et al., 2010; Rohlfing et al., 2011). Primers spanning the 3′ end of the *pgp-3* gene and the 5′ end of the mCherry sequence were utilized to specifically amplify the *pgp-3-mCherry* transgene mRNA. Samples were normalized against expression levels for the actin gene *act-2*. The sequences of qPCR primers are available upon request.

RNAi

RNAi feeding clones were obtained either from the Ahringer library or the ORFeome RNAi collection (Open Biosystems). RNAi bacteria were cultured as previously described (Lamitina, 2006) and seeded onto NGM plates containing 1 mM IPTG. Bacteria were allowed to induce dsRNA for at least 24 hours. For gene knockdowns that were not lethal, hypochlorite-synchronized L1 stage animals were placed onto the RNAi bacteria and were selected for imaging ~24 hours post-L4 stage. For gene knockdowns that produced larval lethality (*sec-23*, *sec-24.1*, *cdc-48.1*, *cdc-48.2* and *rpt-5*), animals were grown on control plates until the L4 stage then transferred to plates containing RNAi bacteria, where they were cultured for 24 hours before imaging.

Protein preparation and western blot analysis

Synchronized young adult worms grown at 20°C on NGM OP50 plates were washed three times with M9 and immediately frozen in liquid nitrogen. Protein extraction was performed by douncing in lysis buffer [100 mM Tris-Cl, pH 8.0; 50 mM NaCl; 100 mM sucrose; 1 mM EDTA and Protease inhibitor cocktail (Roche)]. The resulting worm lysate was centrifuged at 5800 ***g*** for 10 minutes at 4°C to generate a low speed pellet and low speed supernatant. The low speed supernatant was then centrifuged at 100,000 ***g*** for 1 hour at 4°C to generate a high speed supernatant and high speed pellet. The high speed supernatant (cytoplasm) was collected and the high speed pellet (membranes) was resuspended with Tris buffer containing 0.1% Triton X-100. The protein concentration of each sample was determined using the BCA method (Pierce) and identical amounts of protein were loaded for western assays. The difference between PGP-3^{wt} and PGP-3$^{\Delta F508}$ could be observed in crude worm lysates, low-speed supernatants and high-speed pellets (data not shown). Data in all figures show the high speed pellet fraction, because this fraction gave the most consistently even gel loading based on total protein levels and loading controls. The 3×FLAG epitope was detected using anti-3×FLAG (Sigma Chemical Co., M2 clone). The mCherry epitope was detected using an anti-mCherry (Clontech) antibody. Anti-VHA-5 (Vacuolar H ATPase) and anti-HSP-90 were used as loading controls for membranes and cytosol, respectively. Secondary antibodies used were anti-mouse HRP (as above) and anti-rabbit HRP (1:5882 dilution; Amersham). Bands were visualized with a Thermo Scientific chemiluminescent substrate detection system (Prod. #34080).

Microscopy

Young adult animals (24 hours post-L4 stage, unless otherwise indicated) were anesthetized with 10 mM levamisole, mounted on a 2% agarose pad and fluorescently imaged with an inverted wide-field microscope (Leica DMI4000). For deconvolved images, a Z-stack through the intestine, centered on the intestinal lumen, was acquired in 0.2 µ steps using a 1.40 NA Plan Apo 63× lens. Deconvolution was implemented through Leica AF6000 software and utilized the nearest-neighbor method and five to ten iterations. For image quantification, only raw, non-deconvolved images were utilized. In order to reduce the effects of sample photobleaching, the focal plane was first centered on the lumen of the intestine containing the apical membrane using DIC. Samples were then immediately imaged in the mCherry channel at the same single focal plane. For all images within an experiment, the exposure settings were identical between *pgp-3*^{wt} and *pgp-3*$^{\Delta F508}$ animals.

Quantification

Leica AF6000 software was used to measure mCherry fluorescence of images. Apical membrane fluorescence was determined by measuring the average pixel intensity along the length of the apical membrane of worms imaged in the mCherry channel, using the linear quantification feature of the software. For each image, a line

TRANSLATIONAL IMPACT

Clinical issue

Cystic fibrosis (CF) is a genetically inherited disease that disrupts epithelial cell function. Most cases of CF are caused by the deletion of a single amino acid (ΔF508) in the cystic fibrosis transmembrane conductance regulator (CFTR) protein, which is a cAMP-regulated Cl^- channel and member of the ABC transporter gene family. The ΔF508 mutation disrupts the ability of CFTR to fold in the endoplasmic reticulum (ER). As a result, $CFTR^{\Delta F508}$ fails to traffic to the apical membrane of epithelial cells, which impairs transcellular salt and water movement in absorptive and secretory epithelial tissues. Certain manipulations (such as osmotic adaptation, inhibition of ER quality control pathways) allow $CFTR^{\Delta F508}$ to reach the membrane, where it can function as a Cl^- channel and promote salt and water movement. Although several animal models of $CFTR^{\Delta F508}$ misfolding (including mice, pigs and ferrets) exist, these systems do not permit rapid genetic dissection of the pathways contributing to ΔF508-dependent pathophysiology.

Results

To complement studies of mammalian $CFTR^{\Delta F508}$, the authors developed a fluorescence-based *C. elegans* model of ΔF508-dependent protein destabilization. Although worms do not express CFTR, they do express closely related ABC transporters called P-glycoproteins. Introduction of the ΔF508 mutation into the *C. elegans* P-glycoprotein PGP-3 post-transcriptionally destabilized the protein and inhibited its trafficking to the apical membrane of epithelial cells. Similar to mammalian cells, activation of the osmotic stress response or inhibition of *C. elegans* ER quality control proteins stabilized $PGP\text{-}3^{\Delta F508}$ and increased the levels of protein at the apical plasma membrane.

Implications and future directions

This model will allow, for the first time, the use of unbiased forward and reverse genetic approaches in a live-animal setting to identify regulators of ΔF508-dependent protein destabilization. Such regulators can be easily identified in live animals as mutants that increase the abundance and/or apical membrane localization of the $PGP\text{-}3^{\Delta F508}$ protein, as measured by fluorescence. Homologs of these genes in humans could represent new drug targets for the treatment of CF. Additionally, polymorphisms in these genes could influence the timing and/or severity of CF disease in humans.

was traced along the length of the apical membrane, and average pixel intensity along the line was recorded. The apical membrane of cells on both sides of the lumen was measured, and the average pixel intensity was used. Total intestinal fluorescence was determined by measuring the average pixel intensity of the intestine of worms imaged in the mCherry channel, using the area quantification feature of the software. For each image sampled, a region of interest was selected by tracing the basolateral sides of the intestinal wall. For each strain, the average pixel intensity (apical or total) of the test group was normalized to the readings obtained from the control group.

Statistics

All data are presented as means ± standard deviations. For pairwise comparisons, we used the Student's *t*-test. For multiple comparisons testing, we used the ANOVA test with the Dunnet's post-hoc test for significance. *P*-values of <0.05 were taken to indicate statistical significance.

ACKNOWLEDGEMENTS

Some nematode strains used in this work were provided by the *Caenorhabditis* Genetics Center, which is funded by the NIH National Center for Research Resources (NCRR). We thank Michel Labouesse for the kind gift of the VHA-5 antibody and Meera Sundaram for the kind gift of the HSP90 antibody.

COMPETING INTERESTS

The authors declare that they do not have any competing or financial interests.

AUTHOR CONTRIBUTIONS

All authors conceived, designed and performed the experiments, analyzed the data and wrote the paper.

FUNDING

This work was supported by a pilot grant from the University of Pennsylvania Cystic Fibrosis Research Center (to T.L.) and a grant from the National Institutes of Health [1R01AA017580 to T.L.]. J.S. was supported by a grant from the National Institutes of Health [K12-GM-081259].

SUPPLEMENTARY MATERIAL

Supplementary material for this article is available at http://dmm.biologists.org/lookup/suppl/doi:10.1242/dmm.008987/-/DC1

REFERENCES

Allman, E., Johnson, D. and Nehrke, K. (2009). Loss of the apical V-ATPase a-subunit VHA-6 prevents acidification of the intestinal lumen during a rhythmic behavior in C. elegans. *Am. J. Physiol.* **297**, C1071-C1081.

Barlowe, C., Orci, L., Yeung, T., Hosobuchi, M., Hamamoto, S., Salama, N., Rexach, M. F., Ravazzola, M., Amherdt, M. and Schekman, R. (1994). COPII: a membrane coat formed by Sec proteins that drive vesicle budding from the endoplasmic reticulum. *Cell* **77**, 895-907.

Brenner, S. (1974). The genetics of Caenorhabditis elegans. *Genetics* **77**, 71-94.

Brignull, H. R., Morley, J. F., Garcia, S. M. and Morimoto, R. I. (2006). Modeling polyglutamine pathogenesis in C. elegans. *Methods Enzymol.* **412**, 256-282.

Brodsky, J. L. and Wojcikiewicz, R. J. (2009). Substrate-specific mediators of ER associated degradation (ERAD). *Curr. Opin. Cell Biol.* **21**, 516-521.

Broeks, A., Janssen, H. W., Calafat, J. and Plasterk, R. H. (1995). A P-glycoprotein protects Caenorhabditis elegans against natural toxins. *EMBO J.* **14**, 1858-1866.

Chen, E. Y., Bartlett, M. C., Loo, T. W. and Clarke, D. M. (2004). The DeltaF508 mutation disrupts packing of the transmembrane segments of the cystic fibrosis transmembrane conductance regulator. *J. Biol. Chem.* **279**, 39620-39627.

Cheng, S. H., Gregory, R. J., Marshall, J., Paul, S., Souza, D. W., White, G. A., O'Riordan, C. R. and Smith, A. E. (1990). Defective intracellular transport and processing of CFTR is the molecular basis of most cystic fibrosis. *Cell* **63**, 827-834.

Cohen, E., Bieschke, J., Perciavalle, R. M., Kelly, J. W. and Dillin, A. (2006). Opposing activities protect against age-onset proteotoxicity. *Science* **313**, 1604-1610.

Dang, H., Klokk, T. I., Schaheen, B., McLaughlin, B. M., Thomas, A. J., Durns, T. A., Bitler, B. G., Sandvig, K. and Fares, H. (2011). Derlin-dependent retrograde transport from endosomes to the Golgi apparatus. *Traffic* **12**, 1417-1431.

Donoso, G., Herzog, V. and Schmitz, A. (2005). Misfolded BiP is degraded by a proteasome-independent endoplasmic-reticulum-associated degradation pathway. *Biochem. J.* **387**, 897-903.

Duret, L. and Mouchiroud, D. (1999). Expression pattern and, surprisingly, gene length shape codon usage in Caenorhabditis, Drosophila, and Arabidopsis. *Proc. Natl. Acad. Sci. USA* **96**, 4482-4487.

Frokjaer-Jensen, C., Davis, M. W., Hopkins, C. E., Newman, B. J., Thummel, J. M., Olesen, S. P., Grunnet, M. and Jorgensen, E. M. (2008). Single-copy insertion of transgenes in Caenorhabditis elegans. *Nat. Genet.* **40**, 1375-1383.

Garcia, S. M., Casanueva, M. O., Silva, M. C., Amaral, M. D. and Morimoto, R. I. (2007). Neuronal signaling modulates protein homeostasis in Caenorhabditis elegans post-synaptic muscle cells. *Genes Dev.* **21**, 3006-3016.

Gidalevitz, T., Krupinski, T., Garcia, S. and Morimoto, R. I. (2009). Destabilizing protein polymorphisms in the genetic background direct phenotypic expression of mutant SOD1 toxicity. *PLoS Genet.* **5**, e1000399.

Goder, V., Carvalho, P. and Rapoport, T. A. (2008). The ER-associated degradation component Der1p and its homolog Dfm1p are contained in complexes with distinct cofactors of the ATPase Cdc48p. *FEBS Lett.* **582**, 1575-1580.

Hegde, R. S. and Ploegh, H. L. (2010). Quality and quantity control at the endoplasmic reticulum. *Curr. Opin. Cell Biol.* **22**, 437-446.

Howard, M., Fischer, H., Roux, J., Santos, B. C., Gullans, S. R., Yancey, P. H. and Welch, W. J. (2003). Mammalian osmolytes and S-nitrosoglutathione promote Delta F508 cystic fibrosis transmembrane conductance regulator (CFTR) protein maturation and function. *J. Biol. Chem.* **278**, 35159-35167.

Hsu, A. L., Murphy, C. T. and Kenyon, C. (2003). Regulation of aging and age-related disease by DAF-16 and heat-shock factor. *Science* **300**, 1142-1145.

Huyer, G., Piluek, W. F., Fansler, Z., Kreft, S. G., Hochstrasser, M., Brodsky, J. L. and Michaelis, S. (2004). Distinct machinery is required in Saccharomyces cerevisiae for the endoplasmic reticulum-associated degradation of a multispanning membrane protein and a soluble luminal protein. *J. Biol. Chem.* **279**, 38369-38378.

Jensen, T. J., Loo, M. A., Pind, S., Williams, D. B., Goldberg, A. L. and Riordan, J. R. (1995). Multiple proteolytic systems, including the proteasome, contribute to CFTR processing. *Cell* **83**, 129-135.

Kelly, S. M., Vanslyke, J. K. and Musil, L. S. (2007). Regulation of ubiquitin-proteasome system mediated degradation by cytosolic stress. *Mol. Biol. Cell* **18**, 4279-4291.

Lamitina, S. T., Morrison, R., Moeckel, G. W. and Strange, K. (2004). Adaptation of the nematode Caenorhabditis elegans to extreme osmotic stress. *Am. J. Physiol.* **286**, C785-C791.

Lamitina, T. (2006). Functional genomic approaches in C. elegans. *Methods Mol. Biol.* **351**, 127-138.

Lamitina, T., Huang, C. G. and Strange, K. (2006). Genome-wide RNAi screening identifies protein damage as a regulator of osmoprotective gene expression. *Proc. Natl. Acad. Sci. USA***103**, 12173-12178.

Lincke, C. R., Broeks, A., The, I., Plasterk, R. H. and Borst, P. (1993). The expression of two P-glycoprotein (pgp) genes in transgenic Caenorhabditis elegans is confined to intestinal cells. *EMBO J.* **12**, 1615-1620.

Link, C. D., Taft, A., Kapulkin, V., Duke, K., Kim, S., Fei, Q., Wood, D. E. and Sahagan, B. G. (2003). Gene expression analysis in a transgenic Caenorhabditis elegans Alzheimer's disease model. *Neurobiol. Aging* **24**, 397-413.

Loo, T. W., Bartlett, M. C. and Clarke, D. M. (2002). Introduction of the most common cystic fibrosis mutation (Delta F508) into human P-glycoprotein disrupts packing of the transmembrane segments. *J. Biol. Chem.* **277**, 27585-27588.

Louie, R. J., Pagant, S., Youn, J. Y., Halliday, J. J., Huyer, G., Michaelis, S. and Miller, E. A. (2010). Functional rescue of a misfolded eukaryotic ATP-binding cassette transporter by domain replacement. *J. Biol. Chem.* **285**, 36225-36234.

Luo, Y., McDonald, K. and Hanrahan, J. W. (2009). Trafficking of immature DeltaF508-CFTR to the plasma membrane and its detection by biotinylation. *Biochem. J.* **419**, 211-219.

Marciniak, S. J. and Ron, D. (2006). Endoplasmic reticulum stress signaling in disease. *Physiol. Rev.* **86**, 1133-1149.

Mori, K. (2009). Signalling pathways in the unfolded protein response: development from yeast to mammals. *J. Biochem.* **146**, 743-750.

Morley, J. F. and Morimoto, R. I. (2004). Regulation of longevity in Caenorhabditis elegans by heat shock factor and molecular chaperones. *Mol. Biol. Cell* **15**, 657-664.

Moronetti Mazzeo, L. E., Dersh, D., Boccitto, M., Kalb, R. G. and Lamitina, T. (2012). Stress and aging induce distinct polyQ protein aggregation states. *Proc. Natl. Acad. Sci. USA* [Epub ahead of print] doi: 10.1073/pnas.1108766109.

Morton, E. and Lamitina, T. (2010). A suite of MATLAB-based computational tools for automated analysis of COPAS Biosort data. *BioTechniques* **48**, xxv-xxx.

Nakatsukasa, K., Huyer, G., Michaelis, S. and Brodsky, J. L. (2008). Dissecting the ER-associated degradation of a misfolded polytopic membrane protein. *Cell* **132**, 101-112.

Nollen, E. A., Garcia, S. M., van Haaften, G., Kim, S., Chavez, A., Morimoto, R. I. and Plasterk, R. H. (2004). Genome-wide RNA interference screen identifies previously undescribed regulators of polyglutamine aggregation. *Proc. Natl. Acad. Sci. USA* **101**, 6403-6408.

Oka, T., Toyomura, T., Honjo, K., Wada, Y. and Futai, M. (2001). Four subunit a isoforms of Caenorhabditis elegans vacuolar H+-ATPase. Cell-specific expression during development. *J. Biol. Chem.* **276**, 33079-33085.

Ostedgaard, L. S., Rogers, C. S., Dong, Q., Randak, C. O., Vermeer, D. W., Rokhlina, T., Karp, P. H. and Welsh, M. J. (2007). Processing and function of CFTR-DeltaF508 are species-dependent. *Proc. Natl. Acad. Sci. USA* **104**, 15370-15375.

Ostedgaard, L. S., Meyerholz, D. K., Chen, J. H., Pezzulo, A. A., Karp, P. H., Rokhlina, T., Ernst, S. E., Hanfland, R. A., Reznikov, L. R., Ludwig, P. S. et al. (2011). The DeltaF508 mutation causes CFTR misprocessing and cystic fibrosis-like disease in pigs. *Sci. Transl. Med.* **3**, 74ra24.

Pagant, S., Kung, L., Dorrington, M., Lee, M. C. and Miller, E. A. (2007). Inhibiting endoplasmic reticulum (ER)-associated degradation of misfolded Yor1p does not permit ER export despite the presence of a diacidic sorting signal. *Mol. Biol. Cell* **18**, 3398-3413.

Pagant, S., Halliday, J. J., Kougentakis, C. and Miller, E. A. (2010). Intragenic suppressing mutations correct the folding and intracellular traffic of misfolded mutants of Yor1p, a eukaryotic drug transporter. *J. Biol. Chem.* **285**, 36304-36314.

Peters, K. W., Okiyoneda, T., Balch, W. E., Braakman, I., Brodsky, J. L., Guggino, W. B., Penland, C. M., Pollard, H. B., Sorscher, E. J., Skach, W. R. et al. (2011). CFTR Folding Consortium: methods available for studies of CFTR folding and correction. *Methods Mol. Biol.* **742**, 335-353.

Prahlad, V. and Morimoto, R. I. (2011). Neuronal circuitry regulates the response of Caenorhabditis elegans to misfolded proteins. *Proc. Natl. Acad. Sci. USA* **108**, 14204-14209.

Prahlad, V., Cornelius, T. and Morimoto, R. I. (2008). Regulation of the cellular heat shock response in Caenorhabditis elegans by thermosensory neurons. *Science* **320**, 811-814.

Rohlfing, A. K., Miteva, Y., Hannenhalli, S. and Lamitina, T. (2010). Genetic and physiological activation of osmosensitive gene expression mimics transcriptional signatures of pathogen infection in C. elegans. *PLoS ONE* **5**, e9010.

Rohlfing, A. K., Miteva, Y., Moronetti, L., He, L. and Lamitina, T. (2011). The Caenorhabditis elegans mucin-like protein OSM-8 negatively regulates osmosensitive physiology via the transmembrane protein PTR-23. *PLoS Genet.* **7**, e1001267.

Sato, S., Ward, C. L., Krouse, M. E., Wine, J. J. and Kopito, R. R. (1996). Glycerol reverses the misfolding phenotype of the most common cystic fibrosis mutation. *J. Biol. Chem.* **271**, 635-638.

Schaheen, B., Dang, H. and Fares, H. (2009). Derlin-dependent accumulation of integral membrane proteins at cell surfaces. *J. Cell Sci.* **122**, 2228-2239.

Sheps, J. A., Ralph, S., Zhao, Z., Baillie, D. L. and Ling, V. (2004). The ABC transporter gene family of Caenorhabditis elegans has implications for the evolutionary dynamics of multidrug resistance in eukaryotes. *Genome Biol.* **5**, R15.

Solomon, A., Bandhakavi, S., Jabbar, S., Shah, R., Beitel, G. J. and Morimoto, R. I. (2004). Caenorhabditis elegans OSR-1 regulates behavioral and physiological responses to hyperosmotic environments. *Genetics* **167**, 161-170.

Stoltz, D. A., Meyerholz, D. K., Pezzulo, A. A., Ramachandran, S., Rogan, M. P., Davis, G. J., Hanfland, R. A., Wohlford-Lenane, C., Dohrn, C. L., Bartlett, J. A. et al. (2010). Cystic fibrosis pigs develop lung disease and exhibit defective bacterial eradication at birth. *Sci. Transl. Med.* **2**, 29ra31.

Sun, X., Sui, H., Fisher, J. T., Yan, Z., Liu, X., Cho, H. J., Joo, N. S., Zhang, Y., Zhou, W., Yi, Y. et al. (2010). Disease phenotype of a ferret CFTR-knockout model of cystic fibrosis. *J. Clin. Invest.* **120**, 3149-3160.

Teem, J. L., Berger, H. A., Ostedgaard, L. S., Rich, D. P., Tsui, L. C. and Welsh, M. J. (1993). Identification of revertants for the cystic fibrosis delta F508 mutation using STE6-CFTR chimeras in yeast. *Cell* **73**, 335-346.

Teem, J. L., Carson, M. R. and Welsh, M. J. (1996). Mutation of R555 in CFTR-delta F508 enhances function and partially corrects defective processing. *Receptors Channels* **4**, 63-72.

Tsui, L. C. (1992). The spectrum of cystic fibrosis mutations. *Trends Genet.* **8**, 392-398.

van Barneveld, A., Stanke, F., Tamm, S., Siebert, B., Brandes, G., Derichs, N., Ballmann, M., Junge, S. and Tummler, B. (2010). Functional analysis of F508del CFTR in native human colon. *Biochim. Biophys. Acta* **1802**, 1062-1069.

Varga, K., Jurkuvenaite, A., Wakefield, J., Hong, J. S., Guimbellot, J. S., Venglarik, C. J., Niraj, A., Mazur, M., Sorscher, E. J., Collawn, J. F. et al. (2004). Efficient intracellular processing of the endogenous cystic fibrosis transmembrane conductance regulator in epithelial cell lines. *J. Biol. Chem.* **279**, 22578-22584.

Vembar, S. S. and Brodsky, J. L. (2008). One step at a time: endoplasmic reticulum-associated degradation. *Nat. Rev. Mol. Cell Biol.* **9**, 944-957.

Wang, J., Farr, G. W., Hall, D. H., Li, F., Furtak, K., Dreier, L. and Horwich, A. L. (2009). An ALS-linked mutant SOD1 produces a locomotor defect associated with aggregation and synaptic dysfunction when expressed in neurons of Caenorhabditis elegans. *PLoS Genet.* **5**, e1000350.

Wang, X., Venable, J., LaPointe, P., Hutt, D. M., Koulov, A. V., Coppinger, J., Gurkan, C., Kellner, W., Matteson, J., Plutner, H. et al. (2006). Hsp90 cochaperone Aha1 downregulation rescues misfolding of CFTR in cystic fibrosis. *Cell* **127**, 803-815.

Ward, C. L., Omura, S. and Kopito, R. R. (1995). Degradation of CFTR by the ubiquitin-proteasome pathway. *Cell* **83**, 121-127.

Wheeler, J. M. and Thomas, J. H. (2006). Identification of a novel gene family involved in osmotic stress response in Caenorhabditis elegans. *Genetics* **174**, 1327-1336.

Wilke, M., Buijs-Offerman, R. M., Aarbiou, J., Colledge, W. H., Sheppard, D. N., Touqui, L., Bot, A., Jorna, H., de Jonge, H. R. and Scholte, B. J. (2011). Mouse models of cystic fibrosis: phenotypic analysis and research applications. *J. Cyst. Fibros.* **10 Suppl. 2**, S152-S171.

Ye, Y., Shibata, Y., Yun, C., Ron, D. and Rapoport, T. A. (2004). A membrane protein complex mediates retro-translocation from the ER lumen into the cytosol. *Nature* **429**, 841-847.

Younger, J. M., Chen, L., Ren, H. Y., Rosser, M. F., Turnbull, E. L., Fan, C. Y., Patterson, C. and Cyr, D. M. (2006). Sequential quality-control checkpoints triage misfolded cystic fibrosis transmembrane conductance regulator. *Cell* **126**, 571-582.

Zhang, L., Button, B., Gabriel, S. E., Burkett, S., Yan, Y., Skiadopoulos, M. H., Dang, Y. L., Vogel, L. N., McKay, T., Mengos, A. et al. (2009). CFTR delivery to 25% of surface epithelial cells restores normal rates of mucus transport to human cystic fibrosis airway epithelium. *PLoS Biol.* **7**, e1000155.

Zhao, Z., Sheps, J. A., Ling, V., Fang, L. L. and Baillie, D. L. (2004). Expression analysis of ABC transporters reveals differential functions of tandemly duplicated genes in Caenorhabditis elegans. *J. Mol. Biol.* **344**, 409-417.

Zhao, Z., Thomas, J. H., Chen, N., Sheps, J. A. and Baillie, D. L. (2007). Comparative genomics and adaptive selection of the ATP-binding-cassette gene family in caenorhabditis species. *Genetics* **175**, 1407-1418.